# Impedance correction for a branched duct in a thermoacoustic air-conditioner

**Carl Howard**

School of Mechanical Engineering, The University of Adelaide, Adelaide, South Australia, Australia

## ABSTRACT

A thermoacoustic air conditioner that utilises a branched duct network is described in this paper. It was found that the standard four-pole methods to describe the acoustics in the branched duct did not match the predictions from finite element analyses. Additional correction terms to describe lumped inertances at the branch connection are required to properly describe the acoustic behaviour of the system. Branched ducts of square, rectangular, triangular, and semi-circular shapes are considered, and the corresponding terms for the lumped impedances are given.

## INTRODUCTION

The focus of this paper is the development of a mathematical model to describe an end-correction factor for a branched duct in a thermoacoustic air-conditioning system proposed by Swift (2002, p195) shown in Figure 1. The system is a novel implementation of a flow-through style thermoacoustic system and comprises two resonating closed-open tubes placed one on top of the other. The purpose for this concept air-conditioner is to eliminate the use of all heat-exchangers, thereby reducing manufacturing costs. The author of this paper is unaware of anyone having built such a device. For more details about the thermoacoustic operation of the air-conditioner, the reader is referred to Swift (2002). The focus of the work presented here is the acoustics within the ducts.

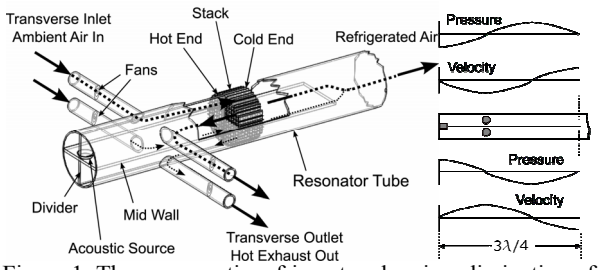


Figure 1: Thermoacoustic refrigerator showing elimination of all heat-exchangers through the use of cross-flow (Swift, 2002).

The upper-half section of the resonating chamber is identical to the lower-half section. Dotted lines are drawn in Figure 1 to show the path of air through the upper-half section. Fans on the 'Transverse Inlet' draw air into the resonating chamber. Within each half section, a vertical divider extends from the end wall to the stack, which forces the air to travel axially along the chamber. The resonating chamber is a closed-open tube and hence the air is forced to move towards the stack. An acoustic driver on the left hand end of the duct provides an oscillating harmonic acoustic pressure and superimposed on the steady cross-flow from the two fan-forced transverse inlets. Fans on the inlet and exhaust tubes attached to the resonator tube are adjusted in such a way that there is a mean flow out the end of the resonator tube. The thermoacoustic effect causes a temperature gradient across the stack, with the end of the stack that is closest to the driver (labelled as 'Hot End' in Figure 1) at a higher temperature than the opposite end of the stack (labelled 'Cold End' in Figure 1). Provided the thermoacoustic system is working correctly, the temperature of the air leaving the cold-end of the device should be lower than the ambient air temperature. The vertical dividing wall forces the air to interact with the stack. Part of the air will be chilled and part of it heated. The dividing wall helps to separate these three streams of air, which are at three different temperatures, in the stack region. A dotted line is shown in the upper-half section Figure 1 pointing from the stack towards the acoustic driver, which indicates the path of the hot-exhaust air-stream leaving the resonance chamber. The acoustic driver placed in the mid-wall acts as an acoustic dipole, as shown in the graphs on the right of Figure 1, as the pressure in the upper tube is 180° out of phase with the pressure in the lower tube. The mid-wall is 3/4 of a wavelength of the acoustic drive frequency, which ensures that the cross-flow streams and cool exit stream are positioned at pressure nodes, to minimise sound transmitted from the cold air duct. Four transverse tubes (two inlets and two outlets) are connected to the resonator tube at a pressure node, permitting ambient air to enter the resonator tube and exhaust the resonator tube at an elevated temperature. These four tubes are positioned at the pressure node to prevent the high-amplitude sound in the resonant cylinder from 'leaking' into the surrounds. Hence, it is important that these tubes are placed precisely at the pressure nodes, and the estimation of the location of this pressure node is part of the focus of this study. It should be noted that during operation of the thermoacoustic air-conditioner, a temperature gradient will exist along the axis of the device. Hence the speed of sound and the corresponding wavelength will also change, thereby altering the location of the pressure node within the cylinder. However, for the work presented here, it is assumed that the speed of sound of the air within the cylinder is constant.

The acoustics of branched ducts is important in applications such as air-conditioning, car manifolds, car exhaust systems, lung function tests, and more recently, using acoustic methods to identify the structures of cave networks. Standard textbooks, such as Blackstock (2000), and Kinsler et al (2000, p290), consider a branched network shown in Figure 2, where an upstream duct of impedance Z1 is bifurcated into two branch impedances Z2 and Z3.

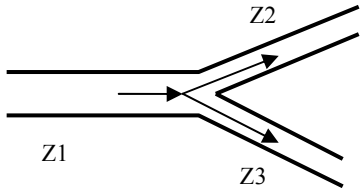


Figure 2: Schematic of a general branched duct.

The combined acoustic impedance is calculated as

$$(1/Z_1) = (1/Z_2) + (1/Z_3) \quad (1)$$

The same result is utilised in four-pole transmission line theory of acoustic ducts (Munjal 1987). Numerous researchers have omitted the impedance at the joint of the branches [Abom 1988, Desantes 2005, Griffin 2000, Boonen 2002, Munjal 1988, Selamet 1997, Blackstock 2000, Kinsler 2000]. It has been found from the work presented here, that an additional 'end-correction' term is required to accurately model the acoustics within the duct network.

Tang (2004) discusses the correction factors for T-branch pipe networks as an additional length correction at the junction. Tang used a finite element method programmed in Matlab to examine various T-branch geometries to determine an effective length correction factors. Unfortunately, the range of dimensions considered did not encompass the dimensions of the problems considered here, and the focus of Tang's work was infinite ducts.

The acoustics of the branched duct considered here is examined using four-pole transmission line theory and is discussed in the next section.

## ACOUSTIC MODEL OF A BRANCHED DUCT

The thermoacoustic system proposed by Swift (2002) can be considered as a branched duct shown in Figure 3, and the equivalent circuit of the duct is shown in Figure 4.

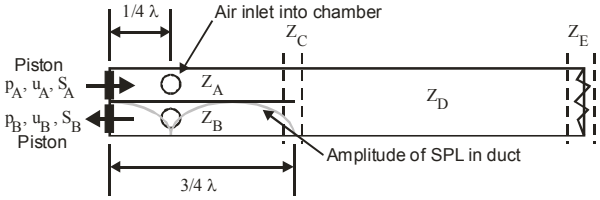


Figure 3: Model of the thermoacoustic branched duct.

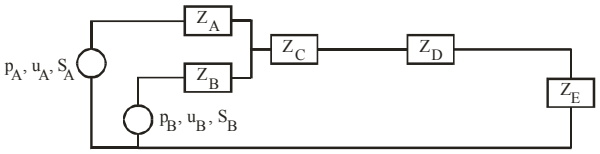


Figure 4: Equivalent circuit of the branched duct.

Piston A provides an acoustic driving volume velocity $U_A$ into the closed-open chamber A. Piston B similarly provides an acoustic driving volume velocity $U_B$ into the closed-open chamber B, but is 180° out of phase with Piston A. The design of the air-conditioner proposes to include transverse inlet and outlet ducts ¼ of a wavelength λ along the duct. In practice, this could introduce an impedance change in the duct. However, for the purposes of the investigation here, the impedances of these side branches shall be omitted from the analysis. It could be considered reasonable to omit the impedance of the branched ducts as the results from analyses of side-branch Helmholtz resonators attached to ducts indicates that if a side branch is placed at a pressure node, as is the case here, the resonator is ineffective at reducing sound transmitted down the duct. Ducts A and B join at 3/4 of a wavelength λ along the duct to Duct D. It has been found from the analyses here, that an additional impedance $Z_C$ is required to account for an additional impedance at the joint. Duct D is assumed to be infinite and has a termination impedance $Z_E$.

The following text contains the derivation of the acoustics of the branched duct presented here using four-pole transmission line theory. Note that the thermoacoustic operation requires that plane wave conditions exist in the duct, and higher-order cross modes do not exist.

At the joint of ducts A and B, there must be pressure continuity, which can be expressed as

$$P_C = P_{AC} = P_{BC} \quad (2)$$

To maintain the volume velocity continuity at the junction, the sum of the volume velocities in the branches must equal the main duct volume velocity, hence

$$V_C = V_{AC} + V_{BC} \quad (3)$$

It is possible to write down four-pole expressions for the pressure and velocity in each of the three ducts as (Beranek & Ver 1992 )

$$\begin{pmatrix} P_A \\ \rho \cdot S_A \cdot U_A \end{pmatrix} = \begin{pmatrix} T_{A11} & T_{A12} \\ T_{A21} & T_{A22} \end{pmatrix} \cdot \begin{pmatrix} P_{AC} \\ \rho \cdot S_{AC} \cdot U_{AC} \end{pmatrix} \quad (4)$$

$$\begin{pmatrix} P_B \\ \rho \cdot S_B \cdot U_B \end{pmatrix} = \begin{pmatrix} T_{B11} & T_{B12} \\ T_{B21} & T_{B22} \end{pmatrix} \cdot \begin{pmatrix} P_{BC} \\ \rho \cdot S_{BC} \cdot U_{BC} \end{pmatrix} \quad (5)$$

$$\begin{pmatrix} P_C \\ \rho \cdot S_C \cdot U_C \end{pmatrix} = \begin{pmatrix} T_{E11} & T_{E12} \\ T_{E21} & T_{E22} \end{pmatrix} \cdot \begin{pmatrix} P_E \\ \rho \cdot S_E \cdot U_E \end{pmatrix} \quad (6)$$

where, ρ is the density of air, $S$ is the cross sectional area of the duct, $U$ is the gas particle velocity, the volume velocity is given by $V_A=\rho S_A U_A$ with similar expressions for $V_B$, $V_C$ $V_{AC}$, $V_{BC}$, the four-pole transfer matrices for the ducts are

$$\begin{pmatrix} T_{A11} & T_{A12} \\ T_{A21} & T_{A22} \end{pmatrix} = \begin{bmatrix} \cos(k \cdot L_A) & j \cdot \left(\frac{c}{S_A}\right) \cdot \sin(k \cdot L_A) \\ j \cdot \left(\frac{S_A}{c}\right) \cdot \sin(k \cdot L_A) & \cos(k \cdot L_A) \end{bmatrix} \quad (7)$$

where $k$ is the wavenumber, $L_A$ is the length of duct A, and similar expressions can be written for $\mathbf{T}_B$ and $\mathbf{T}_E$. Alternatively by pre-multiplying by the inverse of the square matrix in each expression, the expressions can be written as

$$\begin{pmatrix} P_{AC} \\ V_{AC} \end{pmatrix} = \begin{pmatrix} W_{A11} & W_{A12} \\ W_{A21} & W_{A22} \end{pmatrix} \cdot \begin{pmatrix} P_A \\ V_A \end{pmatrix} \quad (8)$$

$$\begin{pmatrix} P_{BC} \\ V_{BC} \end{pmatrix} = \begin{pmatrix} W_{B11} & W_{B12} \\ W_{B21} & W_{B22} \end{pmatrix} \cdot \begin{pmatrix} P_B \\ V_B \end{pmatrix} \tag{9}$$

$$\begin{pmatrix} P_E \\ V_E \end{pmatrix} = \begin{pmatrix} W_{E11} & W_{E12} \\ W_{E21} & W_{E22} \end{pmatrix} \cdot \begin{pmatrix} P_C \\ V_C \end{pmatrix} \tag{10}$$

where the $\mathbf{W}_A$ matrix is the inverse of the $\mathbf{T}_A$ matrix. By using the relationships in Eqs (2) and (3) and after some lengthy algebraic manipulation, it can be shown that the pressures in the ducts are given by the expressions

$$P_A = \frac{\left(-W_{.B11}\cdot T_{.E22}\cdot T_{.E11} + W_{.B11}\cdot T_{.E21}\cdot T_{.E12}\right)}{\left(T_{.E21}\cdot W_{.B11}\cdot W_{.A11} - W_{.A21}\cdot W_{.B11}\cdot T_{.E11} - W_{.B21}\cdot T_{.E11}\cdot W_{.A11}\right)}\cdot V_E \ldots + \frac{\left(W_{.A12}\cdot W_{.B21}\cdot T_{.E11} + W_{.B11}\cdot T_{.E11}\cdot W_{.A22} - W_{.A12}\cdot T_{.E21}\cdot W_{.B11}\right)}{\left(T_{.E21}\cdot W_{.B11}\cdot W_{.A11} - W_{.A21}\cdot W_{.B11}\cdot T_{.E11} - W_{.B21}\cdot T_{.E11}\cdot W_{.A11}\right)}\cdot V_A \ldots + \frac{\left(W_{.B11}\cdot W_{.B22}\cdot T_{.E11} - W_{.B12}\cdot W_{.B21}\cdot T_{.E11}\right)}{\left(T_{.E21}\cdot W_{.B11}\cdot W_{.A11} - W_{.A21}\cdot W_{.B11}\cdot T_{.E11} - W_{.B21}\cdot T_{.E11}\cdot W_{.A11}\right)}\cdot V_B \tag{11}$$

$$P_B = \frac{T_{.E11}\cdot\left(W_{.A22}\cdot W_{.A11} - W_{.A21}\cdot W_{.A12}\right)}{T_{.E21}\cdot W_{.B11}\cdot W_{.A11} - W_{.A21}\cdot W_{.B11}\cdot T_{.E11} - W_{.B21}\cdot T_{.E11}\cdot W_{.A11}}\cdot V_A \ldots + \frac{\left(-T_{.E21}\cdot W_{.B12}\cdot W_{.A11} + W_{.B22}\cdot T_{.E11}\cdot W_{.A11} + W_{.A21}\cdot W_{.B12}\cdot T_{.E11}\right)}{\left(T_{.E21}\cdot W_{.B11}\cdot W_{.A11} - W_{.A21}\cdot W_{.B11}\cdot T_{.E11} - W_{.B21}\cdot T_{.E11}\cdot W_{.A11}\right)}\cdot V_B \ldots + \frac{W_{.A11}\cdot\left(T_{.E21}\cdot T_{.E12} - T_{.E22}\cdot T_{.E11}\right)}{T_{.E21}\cdot W_{.B11}\cdot W_{.A11} - W_{.A21}\cdot W_{.B11}\cdot T_{.E11} - W_{.B21}\cdot T_{.E11}\cdot W_{.A11}}\cdot V_E \tag{12}$$

$$P_E = \frac{\left(W_{.A11}\cdot W_{.B11}\cdot W_{.B22} - W_{.A11}\cdot W_{.B12}\cdot W_{.B21}\right)}{\left(T_{.E21}\cdot W_{.B11}\cdot W_{.A11} - W_{.A21}\cdot W_{.B11}\cdot T_{.E11} - W_{.B21}\cdot T_{.E11}\cdot W_{.A11}\right)}\cdot V_B \ldots + \frac{\left(W_{.A11}\cdot W_{.B11}\cdot W_{.A22} - W_{.A12}\cdot W_{.A21}\cdot W_{.B11}\right)}{\left(T_{.E21}\cdot W_{.B11}\cdot W_{.A11} - W_{.A21}\cdot W_{.B11}\cdot T_{.E11} - W_{.B21}\cdot T_{.E11}\cdot W_{.A11}\right)}\cdot V_A \ldots + \frac{\left(T_{.E12}\cdot W_{.A21}\cdot W_{.B11} + T_{.E12}\cdot W_{.B21}\cdot W_{.A11} - W_{.A11}\cdot W_{.B11}\cdot T_{.E22}\right)}{\left(T_{.E21}\cdot W_{.B11}\cdot W_{.A11} - W_{.A21}\cdot W_{.B11}\cdot T_{.E11} - W_{.B21}\cdot T_{.E11}\cdot W_{.A11}\right)}\cdot V_E \tag{13}$$

The equivalent radius for a non-circular tube is given by Beranek and Ver (1992) as $a = 2S/L_p$, where $L_p$ is the perimeter of the tube. Note that Pierce (1991, p349) approximates it as $a = \sqrt{S/\pi}$. Beranek and Ver (1994, p379) suggest that an end correction impedance can be described as

$$Z = -j\frac{c}{S}\cot(k\Delta l) \tag{14}$$

where $\Delta l$ is an additional length of duct to account for the branch. Pierce (1991, p348) discusses effective neck lengths for Helmholtz resonators, which is an additional length $\Delta l$ that is required to be added to the actual length of a Helmholtz resonator neck to account for the added inertance of entrained fluid. He suggests that the opening of the neck can be considered as pipes with a flanged termination, in which case the additional neck length is $\Delta l$=0.82$a$, or they could be considered as pipes with an unflanged opening, in which case $\Delta l$=0.61$a$. It seems reasonable that these two extremes bound the problem considered here. It was found from the comparison of the results from the ANSYS analysis and the theoretical four-pole model that a suitable end correction factor for this particular design of branched duct is

$$\Delta l = 0.75a \tag{15}$$

The effect of the branch impedance could be considered as an inertance, effectively lengthening the upper and lower sections of the ducts. A transmission matrix $\mathbf{T}_C$ can be written as

$$T_C = \begin{pmatrix} 1 & Z_r \\ 0 & 1 \end{pmatrix} \tag{16}$$

and can be used to modify the response in each duct. Hence the equations for the upper duct A can be written as

$$\begin{pmatrix} P_A \\ \rho\cdot S_A\cdot U_A \end{pmatrix} = \begin{pmatrix} T_{A11} & T_{A12} \\ T_{A21} & T_{A22} \end{pmatrix} \cdot \begin{pmatrix} 1 & Z_r \\ 0 & 1 \end{pmatrix} \cdot \begin{pmatrix} P_{AC} \\ \rho\cdot S_{AC}\cdot U_{AC} \end{pmatrix} \tag{17}$$

and similarly for the lower duct B. Equation (17) can be used to derive a modified four-pole matrix $\mathbf{T}_A$. By using the results in Eqs. (11)-(13) and substituting the known boundary conditions for the volume velocities, the pressures within the duct can be calculated.

## RESULTS

A parametric finite element model of the duct networks considered here was constructed using the ANSYS software package. Ducts with square, rectangular, isosceles triangular and semi-circular cross sections were examined. The 'duct height' $H$ was a parameter in the model and could be varied so that analyses of ducts of various sizes could be investigated.

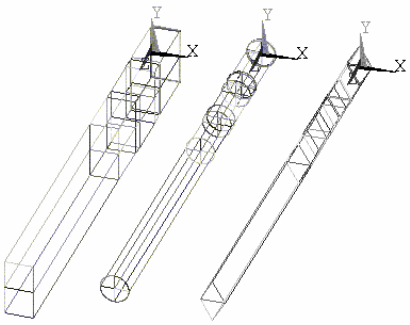


Figure 5: ANSYS models of a square, semi-circular, and triangular duct.

Figure 5 shows ANSYS wire-frame models of the square, semi-circular, and triangular ducts. As an assumption, the frequency used for all analyses was 200Hz, with the density of air $\rho$=1.21kg/m$^3$, the speed of sound fixed at 343m/s, hence the wavelength of sound $\lambda$ was fixed. The overall length of the duct was 1.8$\lambda$, and as described previously, the working resonating section of the duct where the thermoacoustics takes place is 3/4$\lambda$. The end of the duct where the cooled air would exit was modelled as have fully absorptive end-conditions to simulate an anechoic termination. The upper section of the duct was forced with a harmonic volume acceleration of 1m$^3$/s$^2$. Volume acceleration can be converted to an equivalent to the volume velocity by dividing by $j\omega$. The lower section of the duct was forced with the same amplitude of volume acceleration, only 180° out of phase. Figure 6 shows the sound pressure level (SPL), with the contours indicated SPL in dB inside the duct for a square duct with $H$=0.2m. The white contours indicate the loudest SPL and the black contours indicate the lowest SPL. Note that SPL's lower than the minimum contour level are shown as grey! It can be seen that the maximum sound pressure level is at the locations of the acoustic source, labelled as 'MX'. Where the upper and lower ducts join at 3/4$\lambda$ the sound fields cancel and it can be seen that the SPL decays with the minimum SPL labelled 'MN' at the end of duct where the cooled air would exit.

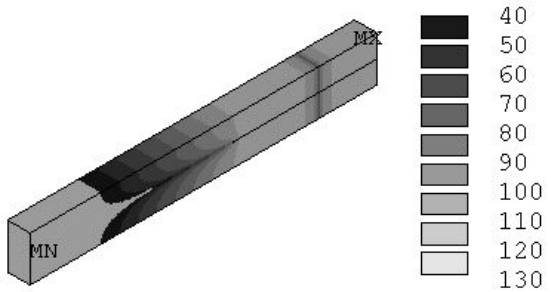


Figure 6: ANSYS results of a semi-infinite branched duct, height = 2 x 0.2m.

Figure 7 shows the results from predictions using ANSYS of the normalised SPL versus the normalised axial distance in a square duct for varying duct heights. The normalised SPL is calculated as the difference in the maximum SPL in the duct and the SPL at an axial position in the duct. The normalised axial position is the axial position along the duct divided by the wavelength. It can be seen that the location of the minimum SPL varies around 1/4λ as the duct height changes.

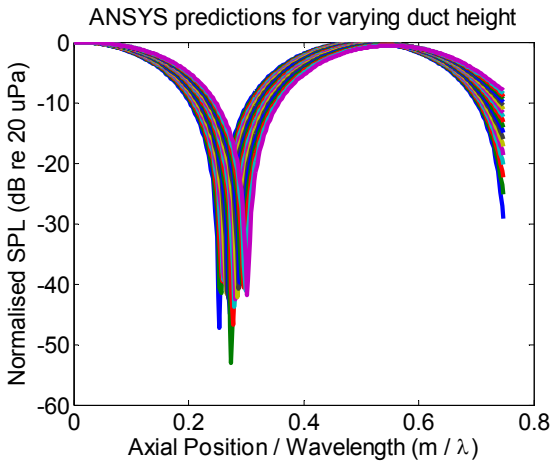


Figure 7: Sound pressure level in ducts of varying height.

Theoretical predictions were made using the four-pole model described here and compared with the results from the finite element modelling. For the theoretical predictions, the equivalent radii of the openings used in the calculations are listed in Table 1.

**Table 1**. Values used for radius and area

| | Radius | Area |
|---|---|---|
| Square | $a=2S/L_p=H/2$ | $H^2$ |
| Semi-circle | $a=H/2$ | $\pi H^2/8$ |
| Triangle | $a=H/2$ | $(H \cos 30)^2 \sqrt{3}/4$ |
| Rectangle | $a=H/2$ | $2H^2$ |

Figure 8 shows the comparison of the position of the minimum SPL in the duct versus the duct height, predicted using the ANSYS software and shown as the point markers, and predicted using the theoretical model and shown as the lines. Note that the term 'duct height' $H$ has different meanings for each duct shape, and the relationship between the duct height and area is described in Table 1. It can be seen that all the results for the ANSYS predictions are very similar, and likewise the results for the theoretical predictions are also very similar. An additional line is drawn in Figure 8 for the theoretical prediction of the position of the minimum SPL in the duct if the correction factor proposed here had not been applied, and is a constant at 1/4λ. The theoretical results presented in Figure 8 can be normalised by the wavelength and are shown in Figure 9.

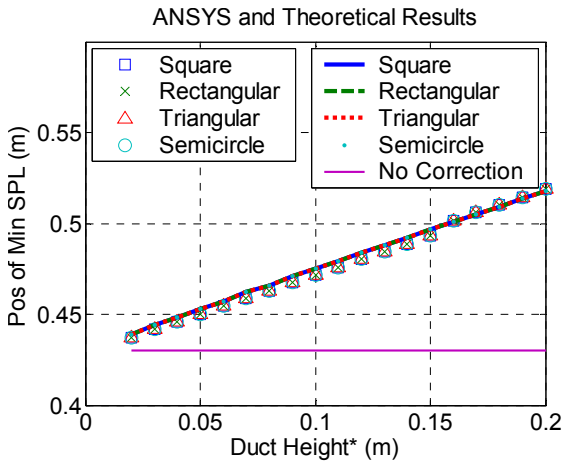


Figure 8: Comparison of ANSYS and theoretical results. The markers indicate predictions using ANSYS and the lines indicate theoretical predictions.

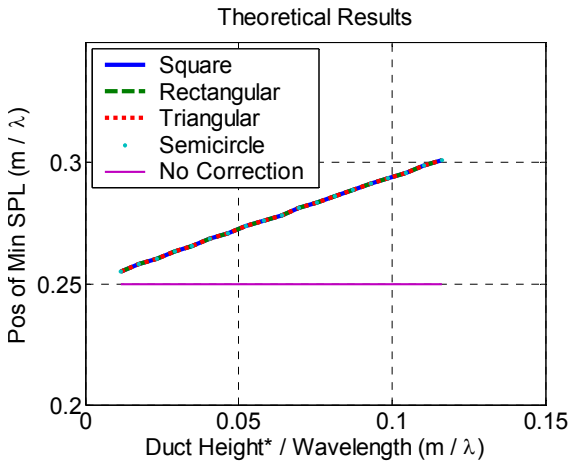


Figure 9: Normalised results from Figure 8.

It should be noted that viscous losses at the pipe openings were not considered in the analyses conducted here, and could be another correction factor that should be included in the theoretical model. It is difficult to model viscous losses in acoustic analyses in ANSYS, hence it was not possible to deduce suitable correction factors for viscous losses.

## CONCLUSIONS

A theoretical model for the acoustics of a branched duct used in a thermoacoustic air-conditioner is presented here. The theoretical model was developed using four-pole transmission line theory. Standard acoustic text books that consider the acoustics of branched ducts require pressure continuity and volume velocity continuity across the joint of the branch, however it was found that does not accurately model the acoustics of the duct. After conducting numerous finite element analyses of the branched duct, it was found that the location of the pressure node within the duct varies with cross sectional area / duct height, whereas conventional four-pole analyses would find that the location is independent of duct height. The results presented here highlight the need to include an additional inertance term at the junction of branched ducts. This additional inertance term was modelled as an end-correction factor for a pipe, and it was found that an end correction length of $\Delta l=0.75a$ resulted in a favourable comparison of theoretical predictions and predictions using ANSYS.

## REFERENCES

Abom, M., Bode, H., and Hirvonen, H., 1988, A simple linear model for the source impedance of an internal combustion engine and manifold, Internoise 88: The Sources of Noise, edited by M. Bockhoff, vol. 3, pp. 1273–1276, International Institute of Noise Control Engineering, Avignon, France.

Beranek, L.L. and Ver, I.L., 1992, Noise and vibration control engineering, principles and applications, John Wiley & Sons.

Blackstock, D.T., 2000, Fundamentals of Physical Acoustics, Wiley-Interscience.

Boonen, R. and Sas, P., 2002, Determination of the acoustical impedance of an internal combustion engine exhaust, Proceedings of ISMA 2002: International Conference on Noise and Vibration Engineering, vol. 5, pp. 1939–1946 (Leuven, Belgium.).

Desantes, J., Torregrosa, A., Climent, H. and Moya, D., 2005, Acoustic performance of a herschel-quincke tube modified with an interconnecting pipe, Journal of Sound and Vibration, 284(1-2), p283–298.

Griffin, S., Huybrechts, S. and Lane, S. A., 2000, Adaptive herschel-quincke tube, Journal of Intelligent Material Systems and Structures, 10 (12), p956 – 961.

Kinsler, L.E., Frey, A.R., Coppens, A.B., Sanders, J.V., 2000, Fundamentals of Acoustics, Fourth Edition, John Wiley and Sons.

Mangiante, G., 2001, The mechanism of active sound absorption in a duct: equivalent circuit analysis, Internoise 2001, edited by R. Boone, paper 13, p. 599, Institute of Noise Control Engineering, The Hague, Holland.

Munjal, M. L., 1987, Acoustics of Ducts and Mufflers With Application to Exhaust and Ventilation System Design, Wiley-Interscience.

Munjal, M. L. and Doige, A. G., 1988, On uniqueness, transfer and combination of acoustic sources in one-dimensional systems, Journal of Sound and Vibration, 121(1), 25–35.

Pierce, A.D., 1989, Acoustics, An introduction to its physical principles and applications, published by the Acoustical Society of America, through the American Institute of Physics, New York.

Selamet, A. and Easwaran, V., 1997, Modified Herschel-Quincke tube: attenuation and resonance for n-duct configuration, Journal of the Acoustical Society of America, 102(1), 164–169.

Swift, G., 2002, Thermoacoustics: A unifying perspective for some engines and refrigerators, Acoustical Society of America.

Tang, S., 2004, Sound transmission characteristics of tee-junctions and the associated length corrections, Journal of the Acoustical Society of America, 115(1), 218 – 227.